International Journal of Architectural, Civil and Construction Sciences
ISSN: 2415-1734
Vol:4, No:3, 2010

Implementation of Generalized Plasticity in Load-Deformation Behavior of Foundation with Emphasis on Localization Problem

A. H. Akhaveissy

Abstract**—**Nonlinear finite element method with eight noded isoparametric quadrilateral element is used for prediction of load-deformation behavior including bearing capacity of foundations. Modified generalized plasticity model with non-associated flow rule is applied for analysis of soil-footing system. Also Von Mises and Tresca criterions are used for simulation of soil behavior. Modified generalized plasticity model is able to simulate load-deformation including softening behavior. Localization phenomena are considered by different meshes. Localization phenomena have not been seen in the examples. Predictions by modified generalized plasticity model show good agreement with laboratory data and theoretical prediction in comparison the other models.

Keywords**—**Localization phenomena, Generalized plasticity, Non-associated Flow Rule

I. Introduction

THE main objective is to implement available model in finite element procedure for load-deformation behavior for geotechnical problems. The parameters for model for sand are derived from laboratories triaxial stress-strain curves under various confining pressures. Then the model is validated at element level by comparison prediction with laboratories data. For practical problems, the models are validated with respect to load-deformation behavior of footing on sand. Footing problem is one of the most highly studied areas in geotechnical engineering.

In the past, constitutive models to analyze geotechnical problems by finite element method were usually based on von Mises and Drucker-Prager criterion (e.g.,[1]-[5]). Although Drucker-Prager and Von Mises model are commonly used, they may not provide sufficient generality in terms of stress path dependency and coupling of volumetric and shear response. Desai, C.S. et al in [3] analyzed footing on artificial material by use of Drucker-Prager, Critical state and modified cap model. They observed that modified cap model provide better results. Faruque and Desai [6] analyzed footing problems as three dimensional by use of a generalized constitutive model. Altaee, A. et al [7] analyzed footing on artificial material by use of bounding surface model. They compared obtained results of bounding surface plasticity model with Drucker-Prager, Critical state and modified cap model. They showed results of bounding surface were better than the other models.

Assistant professor, Department of Civil Engineering, Razi University, Kermanshah-Iran. (Tel: 098 831 4283 264; E-mail:Ahakhaveissy@razi.ac.ir)

Lee and Salgado [8] estimated the bearing capacity of circular footings on sands based on cone penetration test. They used shear elastic modulus in the analysis as a hardening function of second invariant of deviatoric stress to obtain load-deformation curves. In order to describe failure and post-failure soil response, the Drucker-Prager failure criterion was adopted by Lee and Salgado. They obtained load-settlement curves from the finite element analyses for different footing sizes and relative densities (Dr =30, 50, 70 and 90%). The predicted load-settlement curves did not show a limit load. Therefore, they adopted the load at settlement equal to 20% of footing diameter as a limiting bearing capacity of the footing. It was found that both the relative density Dr and the lateral earth pressure ratio K_0 are important factors affecting the load-deformation curves, and the effect of K_0 was greater for lower Dr values. The allowable load at 25 mm settlement was also studied.

In this paper, modified generalized plasticity model is implemented to analyze a footing on sand. The model is able to simulate softening behavior, and prediction of load-deformation behavior of footings comparing with laboratory data.

II. Formulation

For analysis of soil-footing system, generalized plasticity theory is applied by using finite element program in SSINA2D [9] (Soil Structure Interaction Nonlinear Analysis of two dimensional). The formulations used are as follow:

Zienkiewicz, O.C. et al [10] applied bounding surface theory as generalized plasticity theory for analysis of static and transient soil loading. They used critical state yield surface and modified plastic modulus. They defined plastic modulus as product of a function of derivative of yield surface respect to plastic strain and a nonlinear function of distance between current yield surface and bounding surface in bounding surface theory. The same as method for analysis of sand in [11] was used. Chen and Baladi [12] expressed stress-strain relation in terms of the hydrostatic and deviatoric components of strain and stress. Therefore, these relations can be used simply if there are components of flow rule vector and plasticity modulus, then Pastor, M. et al. [13] proposed plastic modulus and flow rule dependent on dilatancy of soil without using special yield and potential surfaces [13]. They defined components of the flow rule in the directions of volumetric and shear deformations. Liu, H. et al [14, 15] proposed some changes in plastic modulus. Here, the relations are reformulated as general and unit vector normal to yield and

potential surface are determined from yield and potential surface. The flow rule was defined in direction of volumetric (n_v) and shear strain (n_s) as [13]:

$$n = (n_v, n_s)$$
$$n_v = \frac{d}{\sqrt{(1+d^2)}} \qquad (1)$$
$$n_s = \frac{1}{\sqrt{(1+d^2)}}$$

Where d is dilation in soil as:

$$d = \frac{d\varepsilon_v^p}{d\varepsilon_s^p} = (1+\alpha)(M-\eta) \quad , \quad \eta = \frac{q}{p} \qquad (2)$$

Mg and M_f are as the slopes defining zero dilatancy in place of M, Figure 1, and α is material parameter. Yield and potential surfaces are found from Eq. (1) by integration as [13]:

$$f = q - M_f * p * (1+1/\alpha) * \left(1 - \left(\frac{p}{p_e}\right)^{\alpha}\right) \qquad (3)$$
$$g = q - M_g * p * (1+1/\alpha) * \left(1 - \left(\frac{p}{p_g}\right)^{\alpha}\right)$$

These surfaces are shown in Figure 1 schematically. where $p = I_1$ and $q = \sqrt{3J_2}$. I_1 and J_2 are first invariant of the stress tensor and second invariant of deviatoric stress tensor, respectively.

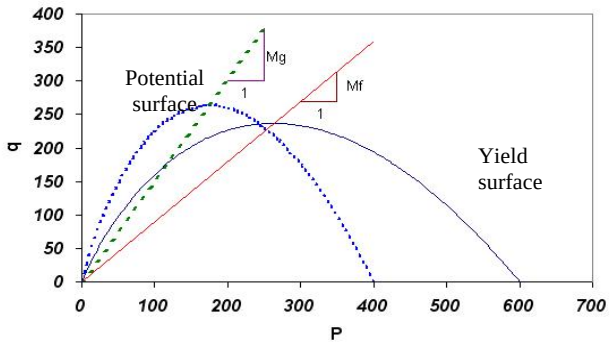

Fig. 1 Schematic yield and potential surfaces

The unit vector normal to yield (f) and potential surface (g) can be defined as

$$n = \frac{\frac{\partial f}{\partial \sigma}}{\left[\frac{\partial f}{\partial \sigma} : \frac{\partial f}{\partial \sigma}\right]^{1/2}} \qquad (4)$$

$$n_{gL} = \frac{\frac{\partial g}{\partial \sigma}}{\left[\frac{\partial g}{\partial \sigma} : \frac{\partial g}{\partial \sigma}\right]^{1/2}}$$

The derivatives in Eq. (4) can be written in as

$$\frac{\partial f}{\partial \sigma} = C_1 \frac{\partial I_1}{\partial \sigma} + C_2 \frac{\partial \sqrt{J_2}}{\partial \sigma} + C_3 \frac{\partial J_3}{\partial \sigma} \qquad (5)$$

J3 is third invariant of deviatoric stress tensor. M_f and Mg depend on Lode's angle [13] but in here, they are assumed as a constant, therefore derivative of yield surface respect to J_3, C_3, is zero.

$$C_1 = \frac{\partial f}{\partial I_1} = (1+\alpha)\left(\frac{M_f}{3} - \frac{\sqrt{3J_2}}{I_1}\right) \qquad (6)$$
$$C_2 = \sqrt{3}$$

If Mg is substituted instead M_f, coefficient C_1 relates to the potential surface. Increment of stress can be determined in finite element method as follow [13]:

$$d\sigma = \left(D_e - \frac{D_e n_{gL/U} . n^T D_e}{H + n^T D_e n_{gL}}\right) d\varepsilon \qquad (7)$$

Where H for loading or reloading:

$$H = H_0 p H_f (H_v + H_s)$$
$$H_f = \left(1 - \frac{\eta}{\eta_f}\right)^4$$
$$\eta_f = \left(1 + \frac{1}{\alpha}\right) M_f \qquad (8)$$
$$H_v = \left(1 - \frac{\eta}{M_g}\right)$$
$$H_s = \beta_0 \beta_1 \exp(-\beta_0 \xi)$$

where ξ is the accumulated deviatoric plastic strain and D_e is elastic constitutive matrix. β_0 and β_1 are material parameters. The expression of H for unloading [13]:

$$H_U = H_{U0}\left(\frac{M_g}{\eta_U}\right)^{\gamma_U} \qquad for \qquad \left|\frac{M_g}{\eta_U}\right| > 1 \qquad (9)$$
$$H_U = H_{U0} \qquad for \qquad \left|\frac{M_g}{\eta_U}\right| > 1$$

where η_U is η for unloading, H_{U0} and γ_U are material parameters. Then, increment of stress can be found by using Eq. (4) to Eq.(9). It must be noted sign of volumetric component of vector perpendicular on potential surface in unloading procedure was altered in accordance to [13] as a constraint, but in present work, in accordance to Eq. (5) and Eq. (6), sign of vector is not changed.

III. Numerical Simulation of Footing Load

The numerical simulation of footing load response and bearing capacity are considered for different sand base on obtained stress-strain curve of triaxial test. In first step, it is analyzed for a footing on artificial soil and the results are compared with observed results in laboratory. In next step,

load-displacement and bearing capacity are determined for a footing on Tehran and Houston sands for different the situ stresses, then a formula is proposed to determine bearing capacity of footing based on the situ stress. The analyses are also implemented by PLAXIS 7.2 which is used for analysis of geotechnical problems.

A. *Footing on artificial sand*

The finite element program is used to analyze the behavior of a model-scale footing. The details of the model-scale footing test were reported in [7]. A rigid rectangular box of size 114×203×876 mm is used as a container. The footing is 76mm wide, 19 mm thick, and 114mm long as shown in Figure 2, is placed at the center of the box. Vertical load is applied on the footing in increments at the center of footing. Measurements are taken for vertical displacements corresponding to each load increment.

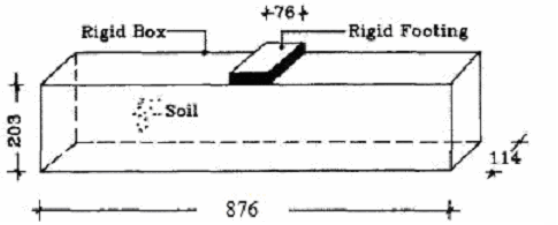

Fig. 2 Layout of model-scale footing ([7]), dimension is mm

Model parameters: In this study, ten model parameters for generalized plasticity model are required to specify the material behavior under generalized three dimensional loading conditions. The model parameters are determined based on conventional triaxial compression test reported in [7] for confining pressure, σ_3, equal to 69 kPa. Obtained results of calibration are compared with observed results in Figure 3 and Table 1 shows the parameters of generalized plasticity model.

TABLE I THE PARAMETERS FOR GENERALIZED PLASTICITY MODEL

E (kPa)	υ	M_f	M_g	H_0	β_0	β_1	α	H_{u_0}	γ_u
15000	0.35	1.0	1.38	125	0.5	0.2	0.4	2000	.005

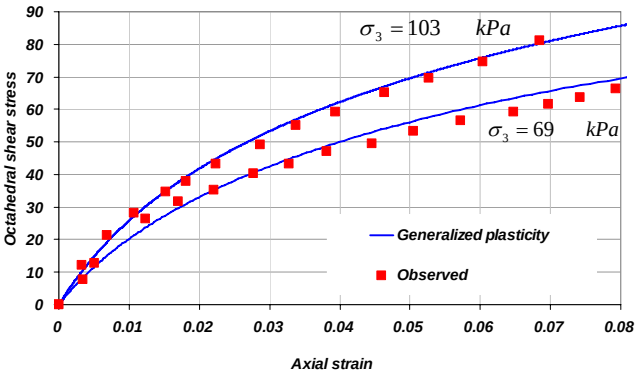

Fig. 3 Comparison predictions and laboratories data for artificial soil

Initial in situ vertical stresses in the soil mass are calculated on the basis of the soil density (2000 kg/m^3). Horizontal stresses are taken equal to vertical stress (K_0=1) as reported in [7], where K_0 is the coefficient of earth pressure at rest. The model scale footing is analyzed with the plain strain idealization. Because of the symmetry, only one half of the soil-footing system is considered. Figure 4 shows the finite element mesh used in the analysis, it consists of 253 eight nodded isoparametric quadrilateral elements, whiles 120 elements was used in [7].

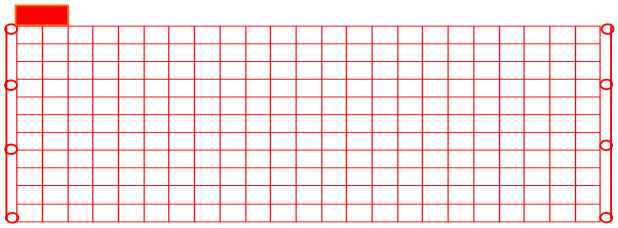

Fig. 4 Finite element mesh for the footing

Finite element results: The observed load-displacement relation of the model-scale footing and the results of the finite element analysis in the present study are Compared in Figure 5. The Figure also includes the results of reported finite element analyses in [7] give same deals of the models used e.g. Critical state, Bounding surface, Drucker-Prager, Modified cap model. Comparisons show that the generalized plasticity model is able to simulate the behavior of the footing-soil system. As illustrated in Figure 5, the best result is obtained from generalized plasticity model. Also Drucker-Prager gives larger limit load and small settlement before limit load and critical state shows stiffer behavior than modified cap model.

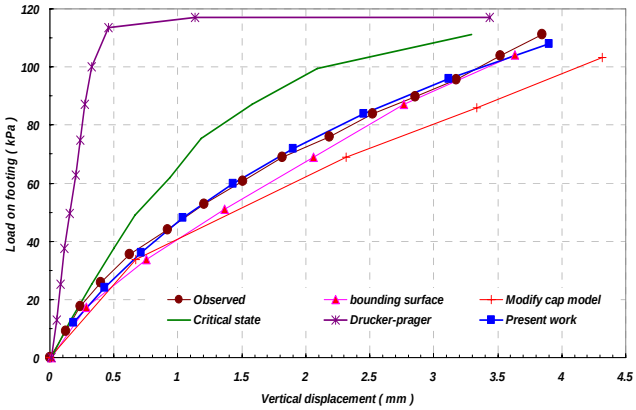

Fig. 5. Comparison of different load-displacement curve

B. *Footing on Tehran sand*

Two cases are considered for Tehran sand. First, strip footing with boundary conditions in Figure 6 is analyzed under concentrated load. This example analyzed by [16] for different material.

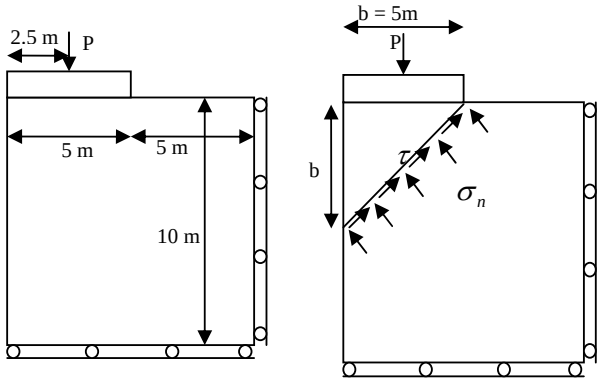

Fig. 6 Boundary conditions and failure line for lower bound

Limit load of footing is obtained by use of Lower bound and Upper bound theorem. Obtained limit loads of Upper bound and Lower bound theorem are the same for this boundary condition. Therefore, appropriate is analytical solution of the example to be compared with numerical solution by use of elastic-perfectly plastic models like Von Mises and Tresca model at first and then comparison with generalized plasticity model in order to considering softening effect and also failure lines for different models are considered. Two different uniform meshes are used for considering of localization phenomena. The mesh a and b are included 16 and 100 elements, respectively.

Lower bound theorem for rigid footing is considered. Limit load in according to Figure 6 is:

$$P = \frac{b\sqrt{2}\tau}{\sqrt{2}} + \frac{b\sqrt{2}\sigma_n}{\sqrt{2}} = b\tau + b\sigma_n$$

$$\tau = \sigma_n = \frac{\sigma_y}{\sqrt{3}}$$

σ_y is yield stress, then

$$P = \frac{2b\sigma_y}{\sqrt{3}} \qquad (10)$$

Numerical solution for different models:

Table 2 shows calibrated parameters for generalized plasticity model. Results of the model by use of Eq. (7) for calibrated parameters in Table 2 are compared with laboratory data [17] and stress-strain curve in accordance to Von-Mises and Tresca models in Figure 7.

TABLE II THE PARAMETERS FOR GENERALIZED PLASTICITY MODEL

P_0 (kg/cm^2)	E (kg/cm^2)	υ	M_f	M_g	H_0	β_0	β_1	α	H_{u0}	γ_u
1	850	0.35	0.75	0.86	270	0.8	0.85	0.34	100	0.1

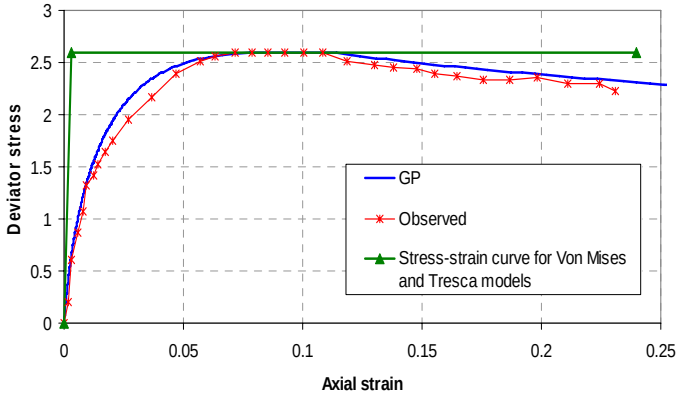

Fig. 7 Comparison of the results for confining pressure equal to 1 kg/cm^2

Elasticity modulus and Poisson ratio are the same as for all of the models and yield stress for Von-Mises and Tresca is 2.6 kg/cm^2 in accordance to Figure 7. Therefore, limit load, Eq. (10), is equal to 1501.11 kg/cm by use of upper or lower bound theorem. Figure 8 shows obtained results for different models by use of the program SSINA2D.

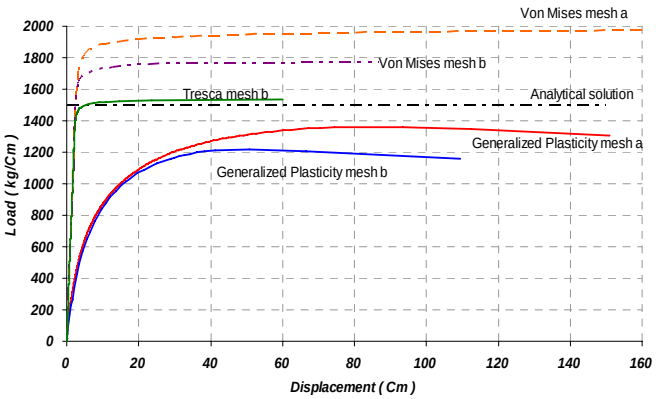

Fig. 8 Load-displacement curve for different models

Comparison limit load for mesh a and b by Von-Mises model with elastic-perfectly plastic behavior show accuracy of results in related to fine and coarse mesh. Obtained limit load of Tresca model and mesh b has good agreement with analytical solution. Therefore, mesh b can be accepted as an appropriation mesh to get exact limit load. Obtained load-displacement curve of generalized plasticity shows effect of softening behavior and also slope of softening branch for mesh a and b are the same. Therefore, localization phenomena have not been seen for different meshes. Amount of limit load was obtained equal to 1200 kg/cm while limit load by upper and lower bound was 1501.11 kg/cm. Figure 9 shows variation of the accumulated deviatoric plastic strain and the deformation for last step analysis of mesh b.

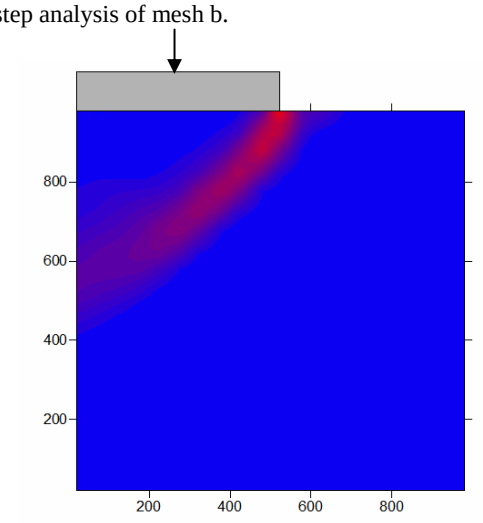

(a)

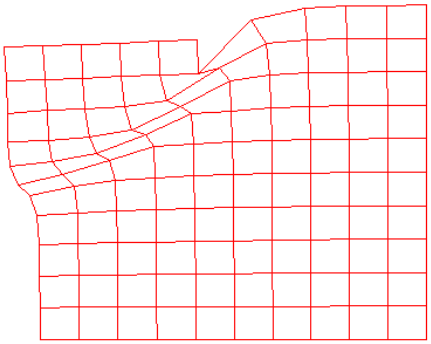

(b)

Fig. 9 (a) Accumulated deviatoric plastic strain and (b) the deformation of the system

Failure line is clear in Figure 9. This failure area is in accordance to failure line of Figure 6 for upper or lower bound theorem. In other words, there is only one failure line according to capability of footing movement. Therefore, obtained results in present work expresses ability of the model and written program. Obtained load-displacement curve of Tresca criterion in Figure 8 has good agreement with analytical solution for mesh b. Therefore, variation of plastic strain in direction of x for Tresca criterion and generalized plasticity are compared in Figure 10.

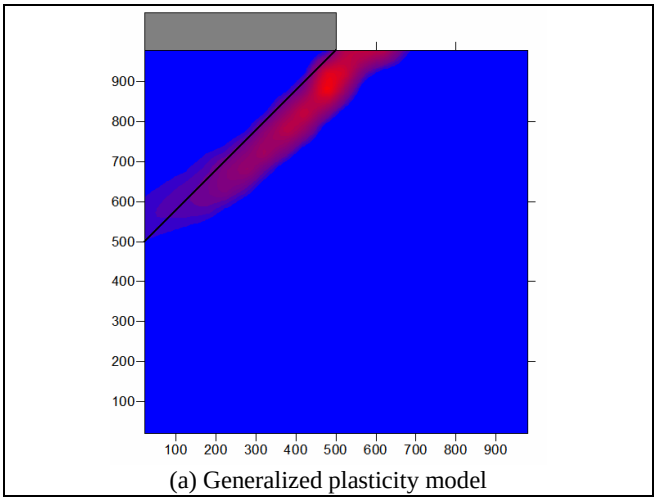

(a) Generalized plasticity model

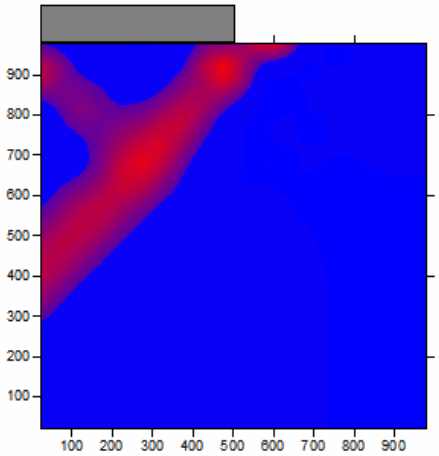

(b) Tresca criterion

Fig. 10 Variation of plastic strain in direction of x, for (a) modified Generalized plasticity and (b) Tresca Criterion

Failure form for Tresca criterion and generalized plasticity are like y and oblique line, respectively. The failure form by Tresca criterion shows a stiff behavior which is clear in Figure 8 for obtained load-displacement curve while obtained failure line by generalized plasticity expresses a true behavior in accordance to ability of movement of system.

IV. Conclusion

Nonlinear finite element method with eight node isoparametric quadrilateral element is used for prediction of load-deformation behavior including bearing capacity of foundations. Generalized plasticity model with non-associated flow rule is used to characterize the constitutive behavior of soils. The model is able to simulate load-deformation including softening behavior. Localization phenomena have

not been seen in the examples. Also Generalized plasticity model is in accordance with theoretical prediction and laboratory data in comparison with Tresca and Von Mises criterions.

REFERENCES

[1] Davidson, H. L. and Chen, W. F. "Nonlinear Response of Undrained Clay to Footings", Computers & structures, 7, pp 539-546, (1977).
[2] Davidson, H. L. and Chen, W. F. "Nonlinear Response of Drained Clay to Footings", Computers & structures, 8, pp 281-290, (1978).
[3] Desai, C. S., Phan, H. V. and Sture, S. "Procedure, Selection and Application of Plasticity Models for a Soil", Int. J. Numer. Anal. Meth, Geomech., 5, pp 295-311, (1981).
[4] Manoharan, N. and Dasgupta, S. P. "Bearing Capacity of Surface Footings by Finite Elements", Computers & Structures, 54 (4), pp 563-586, (1995).
[5] Manoharan, N. and Dasgupta, S. P. "Collapse Load Computation for High-Friction Soil", Computers & Structures, 62 (4), pp 681-684, (1997).
[6] Faruque, M. O. and Desai, C. S. "Implementation of a general Constitutive model for Geological Materials", Int. J. Numer. Anal. Meth. Geomech., 9, pp 415-436, (1985).
[7] Altaee, A., Evgin, E. and Fellenius, B. H. "Finite Element Validation of a Bounding Surface Plasticity Model", Computers & Structures, 42 (5), pp 825-832, (1992).
[8] Lee, J. and Salgado, R. "Estimation of Bearing Capacity of Circular Footings on Sands Based on Cone Penetration Test", Journal of Geotechnical and Geoenvironmental Engineering, 131 (4), pp 442-452 (2005).
[9] Akhaveissy A.H., Desai, C.S., Sadrnejad, S.A., Shakib, H., "Implementation and Comparison of a Generalized Plasticity and Sisturbed State Concept for the Load-Deformation Behavior of Foundation", Transaction D: Civil Engineering Vol.16, No. 3, Sharif University of Technology, Scientia Iranica, June 2009.
[10] Zienkiewicz, O. C., Leung, K. H. and Pastor, M. "Simple Model for Transient Soil Loading in Earthquake Analysis. I. Basic Model and its Application", International Journal for Numerical and Analytical Method in Geomechanics, 9, pp 453-476, (1985).
[11] Pastor, M., Zienkiewicz, O. C. and Leung, K. H. "Simple Model for Transient Soil Loading in Earthquake Analysis. II. Non-Associative Models for Sand", International Journal for Numerical and Analytical Method in Geomechanics, 9, pp 477-498, (1985).
[12] Chen, W. F. and Baladi, G. Y. "Soil Plasticity Theory and Implementation", Developments in Geotechnical Engineering Vol. 38, Elsevier Science Publishers, New York, U.S.A. (1985).
[13] Pastor, M., Zienkiewicz, O. C. and Chan, A. H. C. "Generalized Plasticity and the Modelling of Soil Behaviour", International Journal for Numerical and Analytical Method in Geomechanics, 14, pp 151-190, (1990).
[14] Liu, H. and Ling, H. I. "A Sand Model Based on Generalized Plasticity", 15th ASCE Engineering Mechanics Conference, USA, Columbia University, New York, NY., (2002).
[15] Liu, H. and Song, E. "Seismic Response of Large Underground Structures in Liquefiable Soils Subjected to Horizontal and Vertical Earthquake Excitations", Computers and Geotechnics, 32, pp 223-244 (2005).
[16] O. C. Zienkiewicz, Maosong Huang and M. Pastor, Localization problem in plasticity using finite elements with adaptive remeshing', International Journal for Numerical and Analytical Method in Geomechanics, Vol.19, 127-148, 1995.
[17] Library of Tehran Urban Subway Company reported triaxial test from PEY JOU IRAN consulting engineers for Azadi square in 4m deep.
[18] K. Nesnas& P. Woodward, Advanced braing capacity computation of a footing on sand using a kinematic hardening elstoplastic model, Numerical Model in Geomechanics- NUMOG VII, Pande, Pietruszczak & Schweiger (eds),1999 Balkema, Rotterdam, pp. 463-468.